

Scattering fidelity in elastodynamics

T. Gorin

*Max-Planck-Institut für Physik komplexer Systeme,
Nöthnitzer Str. 38, D-01187 Dresden, Germany*

T. H. Seligman

*Centro de Ciencias Físicas, Universidad Nacional Autónoma de México,
Campus Morelos, C. P. 62251, Cuernavaca, Morelos, México*

R. L. Weaver

*Theoretical and Applied Mechanics, University of Illinois,
104 South Wright Street, Urbana, Illinois 61801, USA*

The recent introduction of the concept of scattering fidelity, causes us to revisit the experiment by Lobkis and Weaver [Phys. Rev. Lett. **90**, 254302 (2003)]. There, the “distortion” of the coda of an acoustic signal is measured under temperature changes. This quantity is in fact the negative logarithm of scattering fidelity. We re-analyse their experimental data for two samples, and we find good agreement with random matrix predictions for the standard fidelity. Usually, one may expect such an agreement for chaotic systems only. While the first sample, may indeed be assumed chaotic, for the second sample, a perfect cuboid, such an agreement is more surprising. For the first sample, the random matrix analysis yields a perturbation strength compatible with semiclassical predictions. For the cuboid the measured perturbation strength is much larger than expected, but with the fitted values for this strength, the experimental data are well reproduced.

Lobkis and Weaver (henceforth LW) experiment [1] have measured the sensitivity of elastic coda waves to temperature changes. After correcting for a trivial term due to change of volume and wavespeed they quantify the effect as “distortion”, and study its decay as a function of time. We shall show that this quantity is the negative logarithm of the “scattering fidelity” introduced and measured in [2, 3]. For sufficiently chaotic dynamics in systems weakly coupled to decay channels, scattering fidelity approaches the standard fidelity amplitude. Fidelity, which is the absolute value squared of the fidelity amplitude, has received a great deal of attention in recent years, as it is used as a benchmark in quantum information processes [4], and in the context of quantum chaos (for a partial overview and references see [5]).

For the above mentioned reasons, we expect the random matrix analysis of fidelity decay [6], to apply to the experiments of LW, as it does in the case of comparable experiments with chaotic microwave cavities [2, 3]. Random matrix theory (RMT) makes a definite statement on the form of the fidelity amplitude as a function of time. It yields a unified description of the “perturbative” and the “Fermi golden rule” [7, 8] regime. This analysis is more appropriate than the treatment in [1], which seems to be on a footing similar to the Fermi golden rule results obtained in [8]. RMT still contains the perturbation strength as a free parameter, which must be determined independently. For quantum chaotic systems, different semiclassical methods have been used [3, 8, 9]. It is still an open problem to extend those results to the perturbative regime [3].

We analyzed the data for two samples, measured by LW, both being three dimensional objects of similar size in all three spatial directions. The first object is the so

called “medium block” (after extra cut) which is supposed to have dominantly chaotic dynamics, with no symmetries left. The second object is a cuboid, called “rectangle”, where the dynamics is not chaotic, but due to mode conversion it is also not integrable and actually known to display random matrix behavior [10]. In both cases, we obtained very good agreement with our RMT result, as far as the form of the scattering fidelity functions is concerned. For the first sample, we also obtain a reasonable agreement for the perturbation strength (comparing the fitted values from an RMT analysis with the theoretical result of LW). For the second sample, we obtain values which are systematically too large, by a factor of two, approximately. Over all, we find that our random matrix approach provides a very good framework, for the discussion of distortion measurements of non-integrable elastodynamic systems, thus providing additional information for the elastic problem. Conversely, experimental results with adequate control of the perturbation strength are rare in fidelity analysis and thus the possibility to use acoustic scattering results is highly welcome.

Scattering fidelity The scattering fidelity [3] is defined as

$$f_{ab}(t) = \langle \hat{S}_{ab}(t)^* \hat{S}'_{ab}(t) \rangle / \sqrt{\langle |\hat{S}_{ab}(t)|^2 \rangle \langle |\hat{S}'_{ab}(t)|^2 \rangle}. \quad (1)$$

Here, $\langle \hat{S}_{ab}(t)^* \hat{S}'_{ab}(t) \rangle$ is the Fourier transform of the cross-correlation function of a scattering matrix element for the unperturbed and perturbed system, respectively. Similarly, $\langle |\hat{S}_{ab}(t)|^2 \rangle$ and $\langle |\hat{S}'_{ab}(t)|^2 \rangle$ are the Fourier transforms of the corresponding autocorrelation functions, used for proper normalization. It can be shown that appropriate averaging (denoted by $\langle \dots \rangle$) yields the stan-

standard fidelity amplitude for chaotic systems weakly coupled to the scattering channels [2]. In that case, a RMT model can be used to compute the fidelity amplitude $f(t)$ on the basis of linear response theory [6]. With $x = t/t_H$ (t_H is the Heisenberg time) and $b_2(x)$, the two point form factor for the Gaussian orthogonal ensemble, one obtains:

$$-\ln f(t) = \lambda_0^2 \left[\frac{x}{2} + x^2 - \int_0^x dx' \int_0^{x'} dx'' b_2(x'') \right]. \quad (2)$$

Here, the ‘‘perturbative’’ and the ‘‘Fermi golden rule’’ regime arise as two particular limits: For small λ_0 the decay of $f(t)$ is dominantly Gaussian, while for large λ_0 it is dominantly exponential [6]. In a microwave experiment excellent agreement between $f_{ab}(t)$ and $f(t)$ has been found [2, 3]. The validity of Eq. (2) for the fidelity of closed chaotic systems has been demonstrated with numerical calculations for the kicked rotor [11].

In [1] the authors measure the acoustic response to a short piezoelectric pulse as a function of time. They consider the normalized cross correlation between two such signals obtained at different temperatures T_1 and T_2 :

$$X(\varepsilon) = \frac{\int dt S_{T_1}(t) S_{T_2}(t(1+\varepsilon))}{\sqrt{\int dt S_{T_1}^2(t) \int dt S_{T_2}^2(t(1+\varepsilon))}}. \quad (3)$$

This equation displays a very similar structure as Eq. (1). The time averaging over a small window, performed in Eq. (3), corresponds to a smoothing of the correlation functions in Eq. (1). The selection of ε , such that the correlation function $X(\varepsilon) = X_{\max}$ becomes maximal, eliminates the trivial effects due to dilation and change of wavespeed, caused by the temperature change. This is quite similar to the spectral unfolding performed in Ref. [2] to eliminate the volume effect of a moving wall. The distortion is defined as $D(t) = -\ln(X_{\max})$, where the time dependence is given by the ‘‘age’’ of the signal, *i.e.* the center of the small time-interval over which the correlation function $X(\varepsilon)$ was evaluated. If formulated as a scattering process, we find $D(t) = -\ln[f_{aa}(t)]$, where the scattering channel a is defined by the transducer, that transmits excitation to and from the sample. Thus, for sufficiently chaotic samples in the elastodynamic scattering experiments, we expect that the scattering fidelity is equal to the fidelity amplitude, and that the latter is well described by the RMT result, Eq. (2).

In [1] the perturbation strength is estimated in terms of the distortion coefficient $C \approx 3.26 \times 10^{-10}/(\text{K}^2 \text{ cm msec}^{-1})$. This value is based on a ray picture of the resonating acoustic waves, the assumption of random reflection angles along the ray paths, and an estimate for the mode conversion rates between dilational and shear waves. We use that value to obtain an estimate for the dimensionless perturbation strength λ_0 in Eq.(2):

$$\lambda_0 = f \sqrt{2c t_H(f)} \quad c = C \Delta^2 V/S, \quad (4)$$

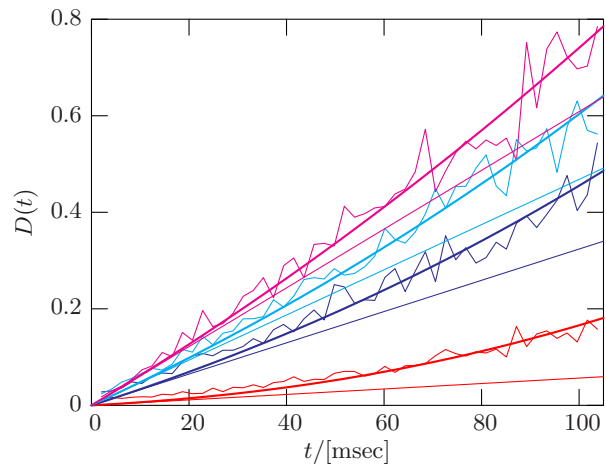


FIG. 1: (Color online) The distortion for the medium block as plotted in Fig. 4 of Ref. [1]. The thin jagged lines correspond to measurements in the frequency ranges 300 kHz, 600 kHz, 700 kHz, and 800 kHz (from bottom to top). The thick lines show $-\ln f(t)$ according to Eq. (2), using the values of λ_0 , as given in Tab. 1 (full RMT fit). For the thin straight lines, only the linear term in Eq. (2) has been taken into account.

where Δ denotes the temperature difference $T_1 - T_2$ in Kelvin, while V and S denote the volume and the surface of the sample. From Refs. [12, 13], we obtain the following expression for the Heisenberg time t_H :

$$t_H = \frac{4\pi}{c_p^3} V (2q^3 + 1) f^2 + \frac{\pi}{2c_p^2} S \left(3q + \frac{2}{q^2 - 1} \right) f. \quad (5)$$

Here, the longitudinal wave velocity is $c_p = 637 \text{ cm/msec}$ and the transverse (shear) wave velocity is $c_s = c_p/q = 316 \text{ cm/msec}$. The frequency (range) is denoted by f .

Medium block: That specimen has volume $V = 906 \text{ cm}^3$ and $S = 636 \text{ cm}^2$, and the temperature difference $\Delta = 4\text{K}$. The distortion, measured as a function of time is shown in Fig. 1. With the Heisenberg times given in Eq. (5), we may fit the perturbation strength λ_0 and compare to the estimate in Eq. (4). For experimental reasons, the data for $D(t)$ is reliable for $t > 20 \text{ msec}$, only. The fits, mentioned above, have been restricted correspondingly.

The agreement between the measured distortions or scattering fidelities and random matrix theory is within the statistical error of the data. A deviation from linear behavior is hardly noticeable, except for the 300 kHz data, which is the only case where $t_H \approx 78 \text{ msec}$ [14] lies within the time range of the figure. However, there is still a considerable effect on the fit values for λ_0 . This can be seen from the dashed curves, which have been obtained by taking only the linear part of Eq. (2) into account.

Tab. 1 gives the values of λ_0 as obtained from linear fits to the data (such a procedure has been applied in [1]), and from fits with the full random matrix result, Eq. (2). In the last column, the respective Heisenberg times are given. In Fig. 2, the fitted perturbation strengths are

f/kHz	λ_0 (lin. fit)	λ_0 (full fit)	t_H/msec
300	0.471	0.298	78.4
600	1.584	1.381	294.6
700	2.136	1.929	397.3
800	2.709	2.505	515.3

TABLE I: Medium block: Table of linear and full RMT fit values for the dimensionless perturbation strength λ_0 together with the respective Heisenberg times for the four frequency ranges, analysed.

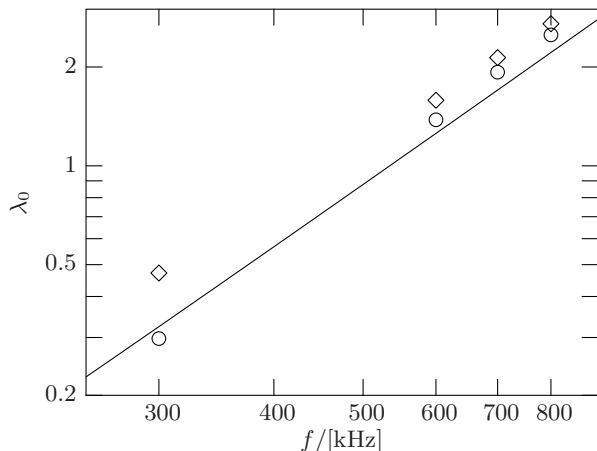


FIG. 2: Medium block: The perturbation strength as a function of the frequency range. The circles show the values for λ_0 obtained from a fit with Eq. (2), while the diamonds show the corresponding values when only the linear term of Eq. (2) is taken into account. The solid line gives the perturbation strength as obtained from Eq. (4).

plotted versus frequency. The solid line shows the estimated behavior of the perturbation strength, computed from Eq. (4). As long as the volume term dominates in the expression (5) for t_H , the perturbation strength increases quadratically with the frequency. The difference between the linear fits (diamonds) and the full RMT fits (circles) is clearly noticeable. The full RMT analysis moves the fit values for λ_0 quite close to the prediction of LW. We have no explanation for the remaining deviations. It is not clear, whether these are statistically acceptable, whether chaoticity is not perfect, or whether there is some other reason. We may recall that in Ref. [3], the experimental perturbation strength did also not agree with the theoretical estimate, as it was too small. However, there, the perturbation strength could be measured independently, from the level dynamics. This demonstrated that for the cavities under study, the semiclassical approximation was not yet justified. It would be desirable, if the level dynamics could be measured in the context of the present experiment.

Rectangle In Fig. 3 and Fig. 4, we analyse data for the rectangle, a perfect cuboid. Clearly, a scalar wave equation would lead to integrable ray dynamics, where our random matrix model must fail. However, in the

f/kHz	λ_0 (lin. fit)	λ_0 (full fit)	t_H/msec
100	0.241	0.061	10.36
200	0.607	0.279	35.75
300	0.903	0.567	76.19
400	1.389	1.033	131.68
500	1.905	1.561	202.21
600	2.564	2.227	287.78
700	3.282	2.957	388.39
800	3.969	3.662	504.04

TABLE II: Rectangle: Table of linear and full RMT fit values for the dimensionless perturbation strength λ_0 together with the respective Heisenberg times.

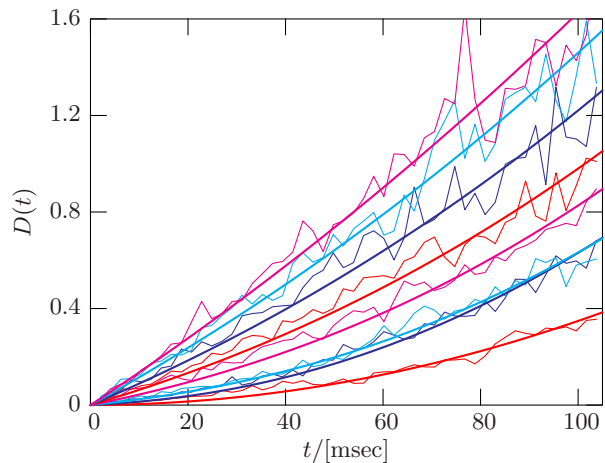


FIG. 3: (Color online) The distortion as a function of time, for the rectangle. The thin jagged lines correspond to measurements in the frequency ranges from 100 kHz to 800 kHz, in steps of 100 kHz (from bottom to top). The thick smooth lines show the best fits with $-\ln f(t)$, according to Eq. (2), with λ_0 given in Tab. 2 (full RMT fit).

present case, the wave field has two components (dilational and a shear waves), which are coupled due to mode conversion. The corresponding classical dynamics are marginally stable, but may still be ergodic. Recently, the elastodynamic system has been studied thoroughly, with a focus on spectral statistics [10]. Apart from certain symmetries, the statistical measures show accurate RMT behavior. Nevertheless, from a theoretical point of view, it remains an open question, whether scattering fidelity still agrees with standard fidelity, and whether the behavior of the fidelity amplitude can be described by random matrix theory. The following analysis with Eq. (2) will shed some light on these questions.

For the rectangle, we have data for eight frequency windows at $f = 100$ kHz, 200 kHz, ..., 800 kHz. The corresponding Heisenberg times range from 10 msec to 500 msec (see Tab. 2). In Fig. 3, one can clearly see a transition from linear to quadratic decay, characteristic for the RMT expression, Eq. (2). Here, it is really surprising that the RMT expression describes the data so

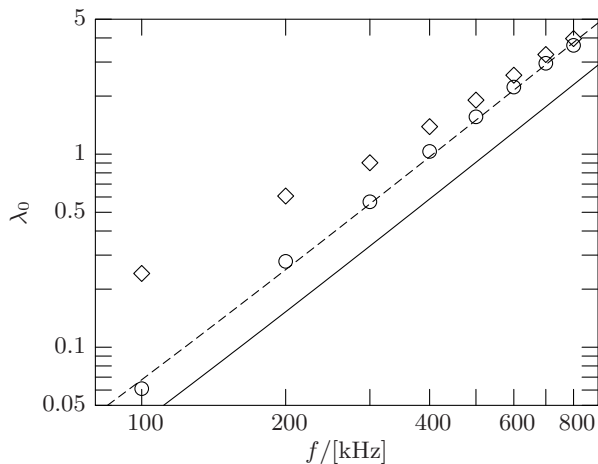


FIG. 4: Rectangle: The perturbation strength as a function of the frequency range. The circles show the values for λ_0 as obtained from Eq. (2), and from the same expression, taking into account only the linear term (diamonds). The solid line gives the perturbation strength as given by Eq. (4). The dashed line shows the same expression, but with $C = 8.90 \times 10^{-10}/(\text{K}^2 \text{ cm msec}^{-1})$ obtained from a fit to the data points (circles).

well. The perturbation strengths obtained from fits to the RMT expression are plotted in Fig. 4 (circles). Except for a constant factor (the distortion coefficient), the result follows the theoretical expectation (Eq. (4), solid line). A fit for the distortion coefficient on the basis of Eq. (4) yields the dashed line. The values for λ_0 obtained from a linear fit (diamonds) clearly, do not follow the theory.

In this work, we identified a previously published elastomechanic scattering experiment as an experiment that measures scattering fidelity in a setting usually called echo dynamics. As in the case of electromagnetic billiards, it turns out that a simple random matrix model describes the decay of the scattering fidelity very well, despite of the fact that these are much more complicated systems. A number of questions could not be answered. In the case of the medium block, we had not enough data, in the low frequency region, where the crossover between Fermi golden rule and perturbative regime occurs. Also, we could not consider any possible symmetries of the system, which might be one source for the remaining differences between estimated and measured perturbation strengths. For the rectangle, our results complement those of [10]. They show that at least in one important aspect the wave functions behave like those of a chaotic system.

The high quality factors of elastomechanic experiments, as well as the possibility to measure explicitly in the time domain, make these experiments particularly attractive. Among possible experiments, we believe that it will be worthwhile to analyze strong perturbation data, *e.g.* larger temperature differences. Such experiments are more difficult, due to precision problems, but may serve to explore the limits of RMT, or detect other regimes of fidelity decay. This is particularly interesting, because the exact solution of the RMT model is now available [15].

We wish to thank O. I. Lobkis for discussions and for data and results put at our disposition. T.H.S. acknowledges financial support under grants CONACyT # 41000-F and UNAM-DGAPA IN-101603. R.L.W. acknowledges support from NSF CMS-0201346.

-
- [1] O. I. Lobkis and R. L. Weaver, *Phys. Rev. Lett.*, **90**, 254302 (2003).
- [2] R. Schäfer, H.-J. Stöckmann, T. Gorin, and T. H. Seligman, Eprint: nlin.CD/0412053 (2004).
- [3] R. Schäfer, T. Gorin, H.-J. Stöckmann, and T. H. Seligman, *New J. Phys.*, **7**, 152 (2005).
- [4] M. A. Nielsen and I. L. Chuang, *Quantum Computation and Quantum Information* (Cambridge University Press, Cambridge, 2000).
- [5] T. Prosen and T. Seligman and M. Žnidarič, *Prog. Theor. Phys. Supp.*, **150**, 200 (2003).
- [6] T. Gorin, T. Prosen, and T. H. Seligman, *New J. Phys.*, **6**, 20 (2004).
- [7] P. Jacquod, P. G. Slivestrov, and C. W. J. Beenakker, *Phys. Rev. E*, **64**, 055203 (2001).
- [8] F. M. Cucchietti, C. H. Lewenkopf, E. R. Mucciolo, H. M. Pastawski and R. O. Vallejos, *Phys. Rev. E*, **65**, 046209 (2002).
- [9] P. Leboeuf and M. Sieber, *Phys. Rev. E*, **60**, 3969 (1999).
- [10] K. Schaadt, A. P. B. Tufaile, and C. Ellegard, *Phys. Rev. E*, **67**, 026213 (2003).
- [11] F. Haug, M. Bienert, W. P. Schleich, T. H. Seligman, and M. G. Raizen, *Phys. Rev. A*, **71**, 043803 (2005).
- [12] M. Dupuis, R. Mazo, and L. Onsager, *J. Chem. Phys.*, **33**, 1452 (1960).
- [13] Y. Safirov and D. Vassiliev, *Spectral Theory of Operators*, edited by S. G. Gindikin, AMS Translations Vol. 2, (American Mathematical Society, 1992).
- [14] According to Lobkis and Weaver, that value is more accurate, than the value given in Ref. [1].
- [15] H.-J. Stöckmann and R. Schäfer, *New J. Phys.*, **6**, 199 (2004).